Surface display for metabolic engineering of industrially important acetic acid bacteria

Marshal Blank[1] and Paul Schweiger[2]

[1] Biology Department, Missouri State University, Springfield, MO, USA
[2] Department of Microbiology, University of Wisconsin-La Crosse, La Crosse, WI, USA

ABSTRACT

Acetic acid bacteria have unique metabolic characteristics that suit them for a variety of biotechnological applications. They possess an arsenal of membrane-bound dehydrogenases in the periplasmic space that are capable of regiospecific and enantioselective partial oxidations of sugars, alcohols, and polyols. The resulting products are deposited directly into the medium where they are easily recovered for use as pharmaceutical precursors, industrial chemicals, food additives, and consumer products. Expression of extracytoplasmic enzymes to augment the oxidative capabilities of acetic acid bacteria is desired but is challenging due to the already crowded inner membrane. To this end, an original surface display system was developed to express recombinant enzymes at the outer membrane of the model acetic acid bacterium *Gluconobacter oxydans*. Outer membrane porin F (OprF) was used to deliver alkaline phosphatase (PhoA) to the cell surface. Constitutive high-strength p264 and moderate-strength p452 promoters were used to direct expression of the surface display system. This system was demonstrated for biocatalysis in whole-cell assays with the p264 promoter having a twofold increase in PhoA activity compared to the p452 promoter. Proteolytic cleavage of PhoA from the cell surface confirmed proper delivery to the outer membrane. Furthermore, a linker library was constructed to optimize surface display. A rigid $(EAAAK)_1$ linker led to the greatest improvement, increasing PhoA activity by 69%. This surface display system could be used both to extend the capabilities of acetic acid bacteria in current biotechnological processes, and to broaden the potential of these microbes in the production of value-added products.

Subjects Biotechnology, Microbiology, Molecular Biology
Keywords Surface display, Fusion linkers, Biocatalysis, Outer membrane proteins, *Gluconobacter oxydans*

INTRODUCTION

Gluconobacter oxydans is an industrially important microbe belonging to the family *Acetobacteriaceae*, commonly referred to as the acetic acid bacteria. *G. oxydans* is an incomplete oxidation specialist known for its ability to partially oxidize alcohols, polyols, and monosaccharides to produce a diverse array of aldehydes, ketones, and organic acids. These reactions occur in the periplasmic space, as *G. oxydans* possesses an arsenal of dehydrogenases bound to the inner membrane. Therefore, industrially valuable

Submitted 21 February 2018
Accepted 26 March 2018
Published 6 April 2018

Corresponding author
Paul Schweiger,
pschweiger@uwlax.edu

Academic editor
Robert Winkler

Additional Information and Declarations can be found on page 16

DOI **10.7717/peerj.4626**

compounds are excreted directly into the growth medium, where they are easily obtained for use as food additives, pharmaceutical precursors, industrial chemicals, and consumer products (*Deppenmeier & Ehrenreich, 2009*; *Deppenmeier, Hoffmeister & Prust, 2002*; *Prust et al., 2005*). What is more, the membrane-bound dehydrogenases are both regiospecific and enantioselective, allowing the microorganism to produce chiral compounds from precursors containing multiple identical functional groups, such as sugars and polyols. Additionally, the membrane-bound dehydrogenases contain prosthetic groups that channel electrons to ubiquinone in the respiratory chain, which facilitates rapid oxidation of substrates (*Deppenmeier & Ehrenreich, 2009*; *Prust et al., 2005*). *G. oxydans* is also osmotolerant and acidophilic, which are desirable industrial characteristics (*Olijve & Kok, 1979*).

Acetic acid bacteria serve many roles in biotechnology, but *G. oxydans* is particularly important (*Deppenmeier, Hoffmeister & Prust, 2002*; *Raspor & Goranovic, 2008*). Currently, *G. oxydans* is used to produce L-sorbose, the precursor to vitamin C (*Pappenberger & Hohmann, 2014*; *Yang & Xu, 2016*) and 6-amino-6-desoxy-L-sorbose, the precursor to the antidiabetic drug miglitol (*Schedel, 2000*). Additionally, this bacterium is used to produce, dihydroxyacetone and erythrulose, which are primarily used as tanning agents in cosmetics (*De Muynck et al., 2007*; *Voss, Ehrenreich & Liebl, 2010*), as well as gluconate and gluconate derivatives, which serve as sequestering agents and drug precursors (*De Muynck et al., 2007*; *Deppenmeier, Hoffmeister & Prust, 2002*). Despite their widespread use in industry, progress toward metabolic engineering of acetic acid bacteria has been partially limited by the lack of molecular tools available for genetic manipulation of this group of microbes (*Kallnik et al., 2010*). Currently, constitutive expression vectors are available for gene expression (*Kallnik et al., 2010*; *Shi et al., 2014*; *Zhang et al., 2010*), and two markerless deletion systems have been developed (*Kostner et al., 2013*; *Peters et al., 2013*). The ability to produce recombinant enzymes for the modification of extracellular substrates has the potential to expand and compliment the natural incomplete-oxidative metabolism of acetic acid bacteria. Signal peptides that allow for periplasmic export are known (*Kosciow et al., 2014*), but the ability to produce additional enzymes bound to the cytoplasmic membrane is limited because this space is already crowded by the large number of native dehydrogenases (*Guigas & Weiss, 2016*). Production of extracellular enzymes is also challenging because *G. oxydans* lacks the machinery to secrete proteins across the outer membrane (*Prust et al., 2005*).

To overcome these limitations, a surface display system for expression of recombinant enzymes at the cell surface of *G. oxydans* and other acetic acid bacteria was designed. This molecular tool enables production of active enzymes with access to the extracellular space, bypassing the crowded inner membrane. Surface display involves translational fusion of a passenger protein with an anchor that innately localizes to the cell surface. Surface display offers several advantages for biocatalysis. Most importantly, substrates do not have to cross membrane barriers to interact with recombinant enzymes, and resulting products are deposited directly into medium, permitting simplified extraction without the need for cell lysis. Additionally, cells can be used for multiple rounds of biocatalysis, as they can be removed from a spent reaction by centrifugation and then resuspended in a

solution containing new substrate. Lastly, surface display eliminates the need to purify enzymes (*Schüürmann et al., 2014*). To this end, a truncated version of outer membrane porin F (OprF) from *Pseudomonas aeruginosa* was translationally fused to alkaline phosphatase (PhoA), from *Escherichia coli*, and activity of the reporter enzyme was quantified in a whole-cell assay. PhoA was proteolytically cleaved from the cell, demonstrating that it was properly delivered to the outer leaflet of the outer membrane. Finally, the surface display system was optimized by testing the effects of various linkers on biocatalysis.

METHODS

Strains and media

Pseudomonas aeruginosa PAO1 (DSMZ 22644) was grown in tryptic soy broth (Becton Dickinson, Franklin Lakes, NJ, USA). *E. coli* 10β (New England Biolabs, Ipswich, MA, USA), herein *E. coli*, was grown in lysogeny broth (1% tryptone, 0.5% yeast extract, 1% NaCl) with 100 μg/mL streptomycin added for strain maintenance. *G. oxydans* 621H, hereafter *G. oxydans*, was grown in yeast mannitol (YM) broth composed of 2% mannitol and 0.6% yeast extract, with 50 μg/mL cefoxitin added for strain maintenance. Plasmids were maintained by addition of 50 μg/mL kanamycin. Electrocompetent *G. oxydans* was prepared by growth in electroporation medium (*Kallnik et al., 2010*). After electroporation, *G. oxydans* cells were plated on yeast glucose calcium carbonate (YGC) agar (2% glucose, 1.5% agar, 0.7% $CaCO_3$, and 0.6% yeast extract) containing cefoxitin and kanamycin.

Materials and molecular techniques

Standard molecular techniques were done according to manufacturer's protocols. Plasmid DNA was extracted using a GeneJet Plasmid Miniprep kit (ThermoFisher Scientific, Waltham, MA, USA) and genomic DNA was extracted using a GenElute Bacterial Genomic DNA kit (Millipore-Sigma, St. Louis, MO, USA). Phusion DNA polymerase and DreamTaq polymerase, FastDigest restriction enzymes, and T4 ligase were purchased from ThermoFisher Scientific (Waltham, MA, USA). Factor Xa protease was purchased from New England Biolabs (Ipswich, MA, USA). Primers were purchased from either Eurofins Genomics (Louisville, KY, USA) or Integrated DNA Technologies (Coralville, IA, USA) (Table 1). DNA sequencing was done by Eurofins Genomics (Louisville, KY, USA).

Construction of a surface display system

The sequence encoding the native signal peptide plus the first 188 amino acids of OprF (OprF188) was amplified from *P. aeruginosa* genomic DNA using primers oprF_F and oprF_R, containing extended *Eco*RI and *Eco*105I restriction sites, respectively. The resulting *oprF188* amplicon was digested with these enzymes and ligated into similarly-cut pBBR1p264-ST and pBBR1p452-ST to produce pBBR1p264-oprF-ST and pBBR1p452-oprF-ST (Table 1). The gene encoding PhoA was amplified from *E. coli* genomic DNA using primers phoA_F and phoA_R, containing extended *Eco*105I and *Hin*dIII sites, respectively. Primer phoA_F was designed to exclude the native periplasmic signal sequence of PhoA. The *phoA* amplicon was digested with *Eco*105I and *Hin*dIII and ligated

Table 1 Plasmids and primers used for molecular cloning.

Plasmid or primer	Description or sequence[a]	Source or restriction site
Plasmids		
pBBR1p264-ST	pBBR1p264 derivative containing a Strep-tag (ST) sequence	*Zeiser et al. (2014)*
pBBR1p452-ST	pBBR1p452 derivative containing a ST sequence	*Kallnik et al. (2010)*
pBBR1p264-oprF-ST	pBBR1p264-ST derivative expressing *oprF188* from *P. aeruginosa*	This study
pBBR1p452-oprF-ST	pBBR1p452-ST derivative expressing *oprF188* from *P. aeruginosa*	This study
pBBR1p264-oprF-phoA	pBBR1p264-oprF-ST derivative with ST removed, expressing *phoA* from *E. coli*	This study
pBBR1p452-oprF-phoA	pBBR1p452-oprF-ST derivative with ST removed, expressing *phoA* from *E. coli*	This study
pBBR1p452-oprF-CL-phoA	pBBR1p452-oprF-phoA derivative with *phoA* removed, replaced by *CL-phoA* encoding a Factor Xa cleavable linker	This study
pBBR1p264-oprF-FL1-phoA	pBBR1p264-oprF-ST derivative with *oprF-ST* removed, replaced by *oprF-FL1* and *FL1-phoA* encoding a $(GGGGS)_1$ flexible linker	This study
pBBR1p264-oprF-FL2-phoA	pBBR1p264-oprF-ST derivative with *oprF-ST* removed, replaced by *oprF-FL2* and *FL1-phoA* encoding a $(GGGGS)_2$ flexible linker	This study
pBBR1p264-oprF-FL3-phoA	pBBR1p264-oprF-ST derivative with *oprF-ST* removed, replaced by *oprF-FL2* and *FL2-phoA* encoding a $(GGGGS)_3$ flexible linker	This study
pBBR1p264-oprF-RL1-phoA	pBBR1p264-oprF-ST derivative with *oprF-ST* removed, replaced by *oprF-RL1* and *RL1-phoA* encoding a $(EAAAK)_1$ rigid linker	This study
pBBR1p264-oprF-RL2-phoA	pBBR1p264-oprF-ST derivative with *oprF-ST* removed, replaced by *oprF-RL2* and *RL1-phoA* encoding a $(EAAAK)_2$ rigid linker	This study
pBBR1p264-oprF-RL3-phoA	pBBR1p264-oprF-ST derivative with *oprF-ST* removed, replaced by *oprF-RL2* and *RL2-phoA* encoding a $(EAAAK)_3$ rigid linker	This study
Primers		
oprF_F	ATGGAATTC**AGGAGG**TAATATTTatgaaactgaagaacaccttaggc	*Eco*RI
oprF_R	ATCGTACGTAACTACCgacgttgtcgcaaacgccgtc	*Eco*105I
phoA_F	AATTTACGTAcctgttctggaaaaccggg	*Eco*105I
phoA_R	ATATAAGCTTtcatttcagccccagagcggc	*Hin*dIII
CL-phoA_F	ATATTACGTA*ATCGACGGCCGC*GGCTCCctgttctggaaaaccgg	*Eco*105I
oprF-FL1_R	AGA*GGATCCGCCGCCGCC*gacgttgtcgcaaacgcc	*Bam*HI
oprF-FL2_R	TAT*GGATCCGCCGCCGCCCGAGCCGCCGCCGCC*gacgttgtcgcaaacgcc	*Bam*HI
oprF-RL1_R	*CTTGGCGGCCGCTTC*gacgttgtcgcaaacgcc	*Not*I
oprF-RL2_R	*CTTGGCGGCCGCTTCCTTCGCCGCGGCTTC*gacgttgtcgcaaacgcc	*Not*I
FL1-phoA_F	*GGCGGCGGCGGATCC*cctgttctggaaaaccgg	*Bam*HI
FL2-phoA_F	*GGCGGCGGCGGATCCGGCGGCGGCGGCTCG*cctgttctggaaaaccgg	*Bam*HI
RL1-phoA_F	*GAAGCGGCCGCCAAG*cctgttctggaaaaccgg	*Not*I
RL2-phoA_F	*GAAGCGGCCGCCAAGGAAGCCGCGGCGAAG*cctgttctggaaaaccgg	*Not*I

Note:
[a] The annealing portion of primers are shown in lowercase, synthetic additions uppercase, restriction sites 2 underlined, linker sequences italicized, and ribosomal binding site bolded.

in-frame into similarly-cut vectors to produce pBBR1p264-oprF-phoA and pBBR1p452-oprF-phoA. Plasmids were transformed into *E. coli* and transformants were screened by colony PCR and confirmed by sequencing. Plasmids were then transformed into *G. oxydans* by electroporation (*Kallnik et al., 2010*; *Kosciow et al., 2016*; *Kostner et al., 2013*). Briefly, 100 mL of electroporation medium was inoculated with an overnight culture of *G. oxydans* and grown to an $OD_{600\ nm}$ of 0.8–1.0. The culture was placed on ice for 20 min,

and chilled cells were harvested by centrifugation at 2,000*g* for 10 min at 4 °C. Cells were washed three times with 50–100% volume of 1 mM HEPES, with centrifugation at 4,000*g* for 10 min at 4 °C. Pellets were resuspended with HEPES and combined into a final volume of 800 μL, to which 200 μL of glycerol was added. Cells were either used immediately or aliquoted, flash-frozen, and stored at −80 °C. For electroporation, 40 μL of electrocompetent cells were combined with 1 μL of plasmid DNA and pulsed with a field strength of 22 kV/cm using a BioRad MicroPulser. After a 6–16 h outgrowth in electroporation medium, transformed cells were plated on YGC agar containing kanamycin and cefoxitin. To incorporate a cleavable linker (CL) into the OprF188-PhoA fusion protein, a 5′-extended version of the PhoA gene, *CL-phoA*, was amplified from *E. coli* genomic DNA using primers CL-phoA_F and phoA_R. Primer CL-phoA_F encoded the amino acid sequence, Ile-Asp-Gly-Arg, recognized by Factor Xa protease (*Nagai & Thogersen, 1987*; *Terpe, 2003*). The *CL-phoA* amplicon was cut with *Eco*105I and *Hin*dIII and ligated into similarly-cut pBBR1p452-oprF-ST to produce pBBR1p452-oprF-CL-phoA (Table 1).

Construction of a linker library for surface display

A library of flexible (FL) and rigid (RL) linkers was assembled similar to *Li et al. (2016)*. The inserts, *oprF-FL1*, *oprF-FL2*, *oprF-RL1*, and *oprF-RL2*, were amplified from the plasmid, pBBR1p264-oprF-ST, using the forward primer, oprF_F, and the respectively-named reverse primers (oprF-FL1_R, oprF-FL2_R, oprF-RL1_R, and oprF-RL2_R) containing either *Bam*HI or *Not*I sites. The inserts, *FL1-phoA*, *FL2-phoA*, *RL1-phoA*, and *RL2-phoA* were amplified from the *E. coli* genome using the reverse primer, phoA_R, and the respectively-named forward primers (FL1-phoA_F, FL2-phoA_F, RL1-phoA_F, and RL2-phoA_F) containing either *Bam*HI or *Not*I sites. The linker system inserts were cut with their corresponding restriction enzymes—all *oprF188* inserts were cut with *Eco*RI, all *phoA* inserts were cut with *Hin*dIII, all FL inserts were cut with *Bam*HI, and all rigid linker (RL) inserts were cut with *Not*I. In parallel, vector pBBR1p264-oprF-ST was cut with *Eco*RI and *Hin*dIII. The linker library inserts were ligated into a linearized vector in a combinatorial fashion to produce six plasmids comprising the linker library: pBBR1p264-oprF-FL1-phoA, pBBR1p264-oprF-FL2-phoA, pBBR1p264-oprF-FL3-phoA, pBBR1p264-oprF-RL1-phoA, pBBR1p264-oprF-RL2-phoA, and pBBR1p264-oprF-RL3-phoA (Table 1).

Phosphatase assays

Alkaline phosphatase assays were done using a modified method of *Kosciow et al. (2014)*. Experimental cultures were inoculated 1:100 from overnight cultures and grown to mid-late exponential phase (OD_{600} of 0.9–1.1 for *E. coli* and 0.6–0.9 for *G. oxydans*). Forty microliters of cells were mixed with 160 μL of substrate buffer (1M Tris base, 10 mM $MnSO_4$, 10 mM $ZnSO_4$, 1.25 mM *p*-nitrophenylphosphate, pH 8.0) in a 96-well microplate. The reactions were incubated with shaking for 60 min at 30 °C and the change of absorbance was monitored at 405 nm in a BioTek EL808 plate reader. Phosphatase activity was reported as absorbance change per hour, normalized by the optical density of the bacterial culture, $\Delta A_{405}/(h \times OD_{600})$.

PhoA localization assay

Localization of the passenger protein was conducted using a modified method *Jiang & Boder (2010)*. YM broth was inoculated 1:100 with an overnight culture of *G. oxydans* harboring plasmid pBBR1p452-oprF-CL-phoA and grown to mid-late exponential phase and 500 µL was centrifuged at 2,000*g* for 5 min. The pellet was resuspended in 200 µL of Factor Xa buffer (100 mM NaCl, 20 mM Tris-base, 2 mM $CaCl_2$, pH 8.0) and Factor Xa protease was added to a final concentration of 20 ng/µL. Samples were incubated overnight at 23 °C with shaking. After incubation, samples were pelleted at 2,000*g* for 5 min, and supernatant was transferred to a new microcentrifuge tube. The supernatant was centrifuged at 16,100*g* for 2 min to remove intact cells and 40-µL aliquots were used to quantify phosphatase activity as described above.

Growth behavior

Yeast mannitol broth was inoculated to an OD_{600} of 0.05 from overnight cultures of *G. oxydans* strains and 1 mL of inoculated broth was added to a 24-well microplate. The plate was incubated at 30 °C with shaking at 150 rpm for up to 24 h, and absorbance was monitored at 595 nm every 5 min in a Flurostar Optima plate reader (BMG Labtech, GmbH, Ortenberg, Germany).

Statistical analysis

R Studio was used to perform statistical analyses and to generate box-and-whisker plots, strip charts, and growth curve graphics (*R Core Team, 2017*). Data were analyzed by performing an analysis of variance and a post-hoc Tukey's HSD test ($q = 0.05$) unless otherwise noted. The R packages used in this study were dplyr, ggplot2, growthcurver, plyr, multcomp, and reshape2 (*Hothorn, Bretz & Westfall, 2008*; *Sprouffske & Wagner, 2016*; *Wickham, 2007*, *2009*, *2011*; *Wickham et al. 2017*).

RESULTS

Surface display in *G. oxydans*

To enable surface display in acetic acid bacteria, a truncated version of OprF (OprF188) was tested for its ability to localize the PhoA reporter enzyme to the cell surface of *G. oxydans*. PhoA was translationally fused to the C-terminal end of OprF188, and the resulting OprF188-PhoA fusion protein was produced via two expression vectors, one containing a high-strength promotor (p264) and the other containing a moderate-strength promotor (p452) (*Kallnik et al., 2010*). As a preliminary test, these surface display constructs were expressed in *E. coli* and phosphatase activity was quantified in a whole-cell assay (Fig. 1). The OprF188-PhoA surface display systems produced statistically significant absorbance changes compared to strains expressing the anchor protein alone when using both the high- ($q < 0.001$) and moderate-strength ($q < 0.001$) promoters, p264 and p452, respectively. Enzymatic rates were approximately sixfold higher in the p264-oprF-phoA system compared to the p452-oprF-phoA system.

In *G. oxydans*, the p264-oprF-phoA strain produced a mean absorbance change of $0.39/(h \times OD_{600})$, corresponding to a volume activity of 3.21 $mU/(mL \times OD_{600})$, which

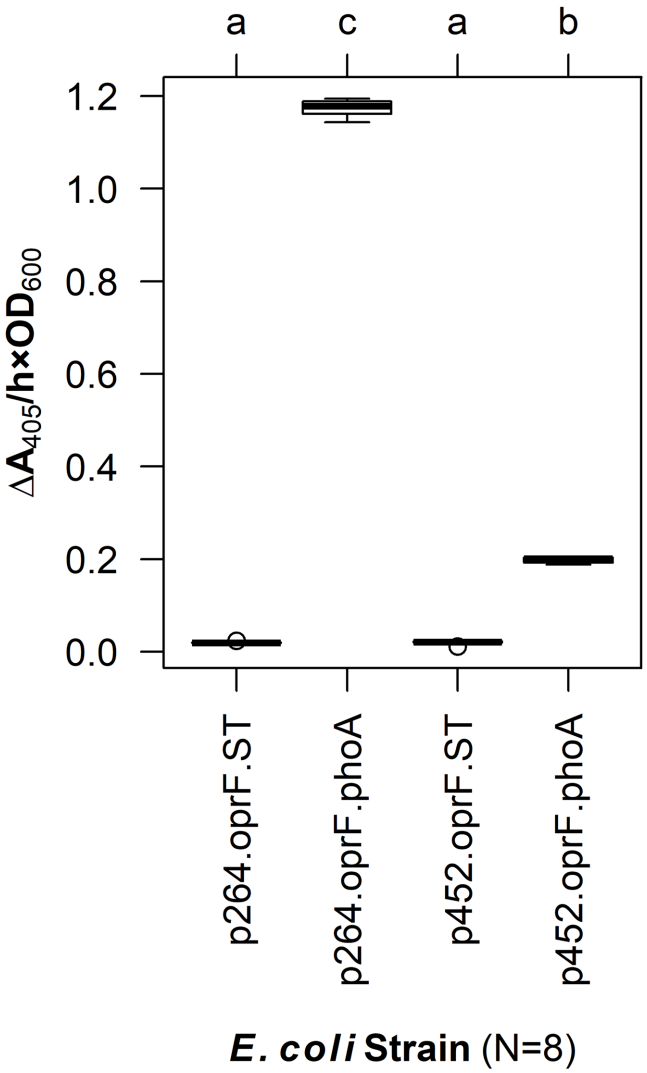

Figure 1 OprF as a surface display anchor in *E. coli*. The OprF188-PhoA fusion protein was produced in *E. coli* using the high-strength (p264) and moderate-strength (p452) promoters. Phosphatase activity was measured in whole-cell reactions. Respective strains producing only the anchor peptide fused to a Strep-tag (ST) served as negative controls. Rate of PhoA activity was monitored as $\Delta A_{405\ nm}/(h \times OD_{600\ nm})$. Letters above the plot denote statistical groups determined by an ANOVA and post-hoc Tukey's HSD test. Full-size DOI: 10.7717/peerj.4626/fig-1

was significantly greater than basal activity ($q < 0.001$) (Fig. 2). This level of activity is approximately threefold lower than that observed when the same construct was expressed in *E. coli*. The p452-oprF-phoA strain produced a mean absorbance change of $0.20/(h \times OD_{600})$ and a volume activity of $1.65\ mU/(mL \times OD_{600})$, which was significantly higher than that of the control ($q < 0.001$). In contrast to the high-strength promotor, there was no reduction in activity when OprF188-PhoA expression was directed by the moderate-strength promoter in *G. oxydans* rather than *E. coli*.

To verify that PhoA was exposed to the extracellular space, a CL was incorporated into the fusion protein sequence. The resulting construct, p452-oprF-CL-phoA, was

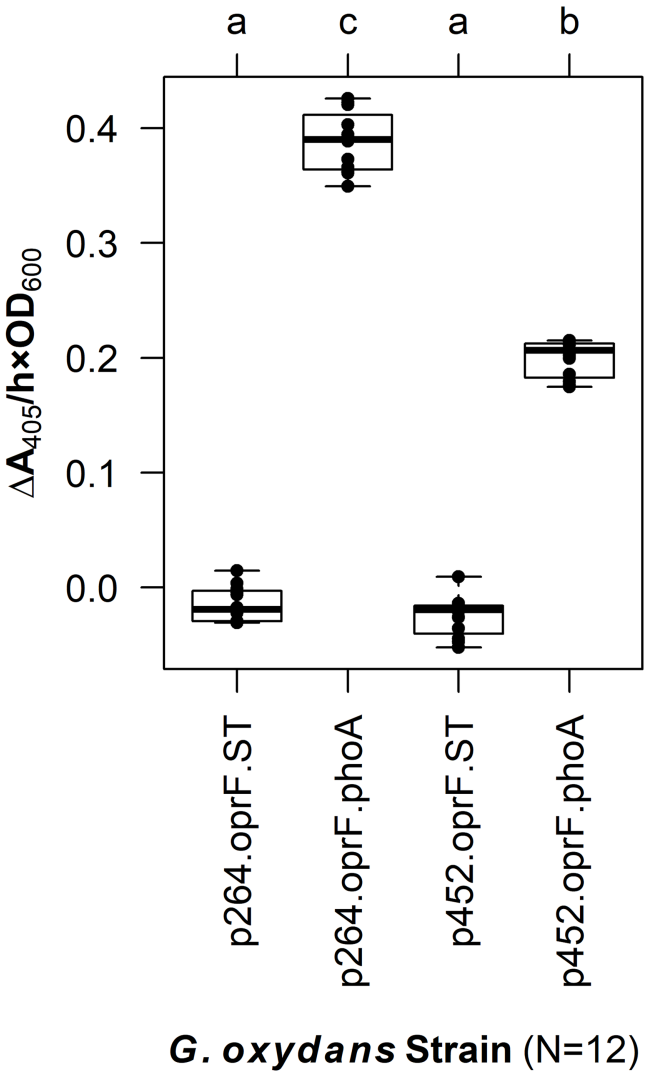

Figure 2 OprF as a surface display anchor in *G. oxydans*. The OprF188-PhoA fusion protein was expressed in *G. oxydans* using the high-strength (p264) and moderate-strength (p452) promoters. Phosphatase activity was measured in whole-cell reactions. Respective strains producing only the anchor peptide fused to a Strep-tag (ST) served as negative controls. Rate of PhoA activity was monitored as $\Delta A_{405\ nm}/(h \times OD_{600\ nm})$. Letters above the plot denote statistical groups determined by an ANOVA and post-hoc Tukey's HSD test. Full-size DOI: 10.7717/peerj.4626/fig-2

transformed into *G. oxydans* and an assay to localize PhoA was done (see Methods). The mean level of phosphatase activity observed in the supernatant from cells treated with Factor Xa protease was higher than that from untreated cells (two-sample *t*-test, $p < 0.001$) (Fig. 3). These data suggest that PhoA was released into the supernatant after cleavage, indicating that PhoA was attached to the outer membrane and oriented toward the medium.

Linker system optimization

To optimize surface display in acetic acid bacteria, a library of linkers was integrated into the OprF188-PhoA surface display systems. First, overhang PCR was used to add linker

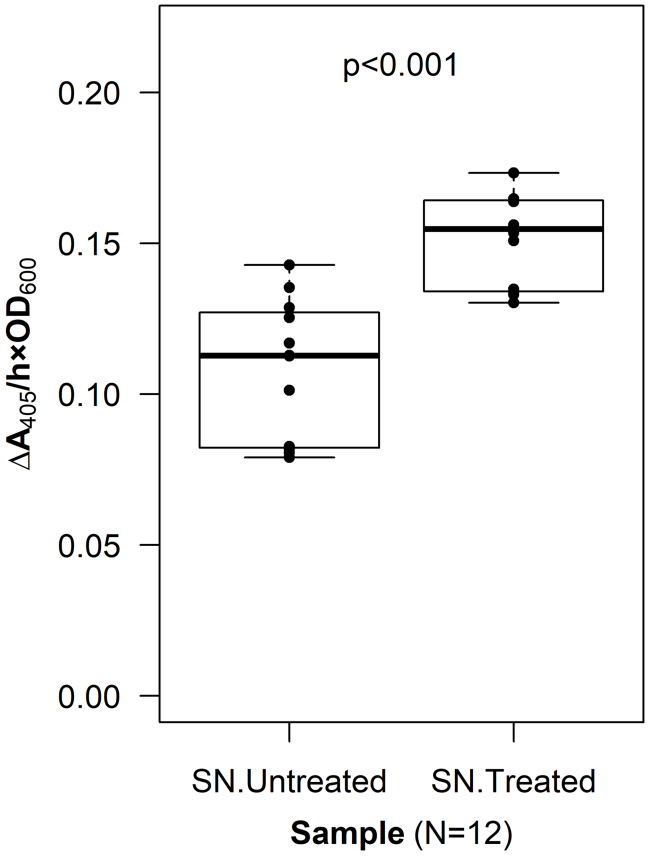

Figure 3 Cleavable linker assay. To confirm proper localization of the passenger enzyme, a cleavable linker motif was incorporated into the OprF188-PhoA surface display system. Whole *G. oxydans* cells were treated with Factor Xa protease and the resulting supernatant (SN) was assayed for phosphatase activity. Rate of PhoA activity was monitored as $\Delta A_{405\ nm}/(h \times OD_{600\ nm})$.

Full-size DOI: 10.7717/peerj.4626/fig-3

building blocks to *oprF188* and *phoA*. These building blocks encoded for either flexible or RLs and contained either *Bam*HI or *Not*I restriction sites, respectively. The modified *oprF188* inserts contained abridged linker sequences at their 3′ ends and the modified *phoA* inserts contained abridged linker sequences at their 5′ ends. Therefore, complete linker sequences resulted from ligation of compatible insert dyads. The building blocks were assembled into the expression vector that showed the highest activity to create six constructs encoding fusion proteins varying in linker composition and linker length: Three containing FLs (FL1, FL2, and FL3) composed of a $(GGGGS)_{1–3}$ motif, and three containing RLs (RL1, RL2, and RL3) composed of the $(EAAAK)_{1–3}$ motif.

The linker library was first expressed in *E. coli* and PhoA activity was quantified (Fig. 4). The FLs had slight negative effects on enzyme activity. While there was no difference between the control lacking a linker and the fusion protein containing the small FL (FL1) ($q = 0.939$), the medium (FL2), and large (FL3) FLs led to a slight but statistically significant decrease in activity ($q < 0.001$ for each). In contrast, the small (RL1) and medium (RL2) RLs did not have any effect on activity ($q = 0.071$ and 0.969, respectively).

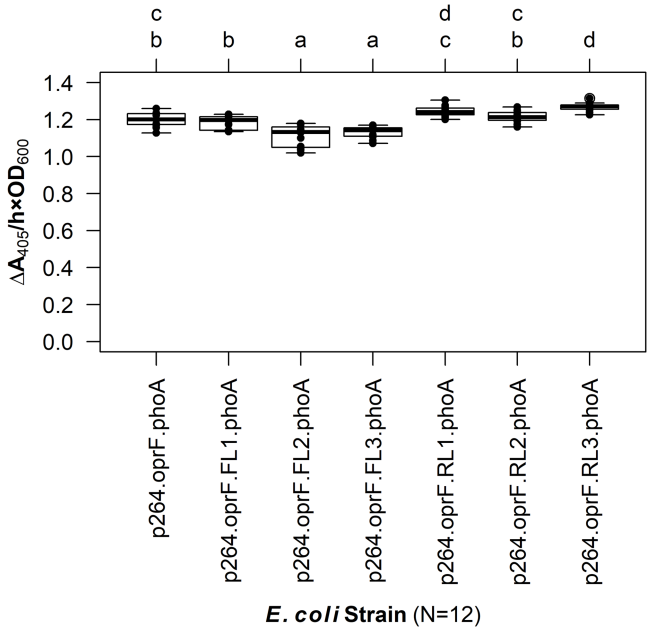

Figure 4 The effects of linkers on biocatalysis in *E. coli*. To determine the effects of linkers on the surface display system, a library of flexible $(GGGGS)_{1–3}$ and rigid $(EAAAK)_{1–3}$ linkers was integrated into the OprF188-PhoA fusion protein and PhoA activity was measured. Rate of PhoA activity was monitored as $\Delta A_{405\ nm}/(h \times OD_{600\ nm})$. Letters above the plot denote statistical groups determined by an ANOVA and post-hoc Tukey's HSD test. Full-size DOI: 10.7717/peerj.4626/fig-4

The large RL (RL3) led to a slight but statistically significant increase in enzymatic activity when compared to the control ($q < 0.001$). However, there was no difference between the RL1 strain and the RL3 strain ($q = 0.692$), suggesting that the higher activity observed for the RL3 strain was likely not biologically significant.

The linker systems had more pronounced effects on PhoA activity in *G. oxydans* compared to the subtle effects of the flexible and RLs in *E. coli* (Fig. 5). While the small FL (FL1) and the medium RL (RL2) had no effect on activity when compared to the control lacking a linker ($q = 0.967$ and $q = 0.765$, respectively), the large RL (RL3) led to a 32% reduction in activity ($q < 0.001$). Interestingly, the small RL (RL1) drastically improved PhoA activity ($q < 0.001$), having a 69% increase in biocatalysis that corresponded to a volume activity of 5.42 mU/(mL × OD_{600}). Attempts to transform plasmids p264-oprF-FL2-phoA and p264-oprF-FL3-phoA into *G. oxydans* were unsuccessful, suggesting that the medium (FL2) and large (FL3) FLs were toxic at high expression.

Effect of surface display on growth of *G. oxydans*

To characterize the effects of protein production and surface engineering on the growth behavior of *G. oxydans* cells, a method was developed to follow the growth of recombinant *G. oxydans* strains using standard 24-well microplates, allowing automated monitoring of cell growth in a plate reader. Strains containing OprF188 surface display systems were compared to wildtype *G. oxydans* 621H growth (Fig. 6). When the high-strength p264 promoter was used, production of the OprF188 anchor protein without fusion to PhoA

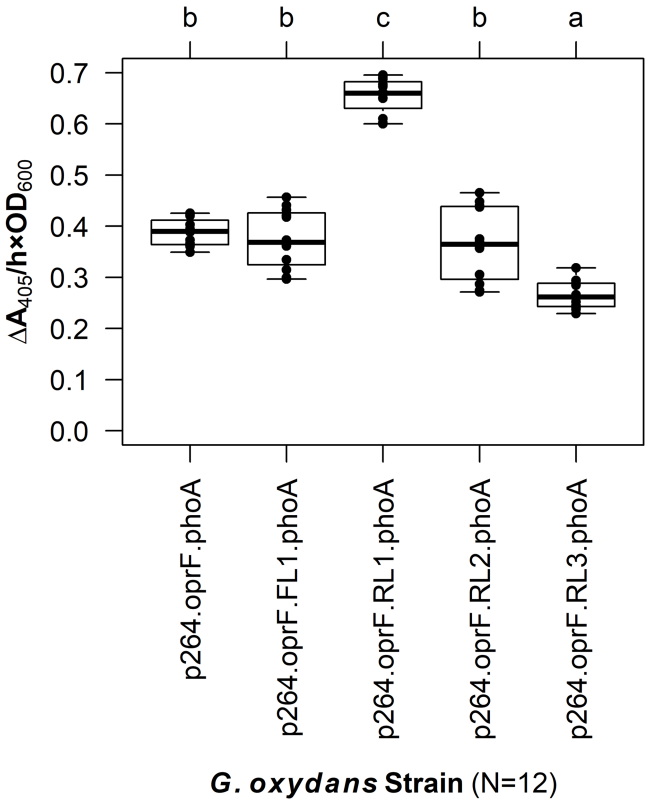

Figure 5 The effects of linkers on biocatalysis in *G. oxydans*. A linker library consisting of flexible $(GGGGS)_1$ and rigid $(EAAAK)_{1–3}$ linkers was integrated into the OprF188-PhoA fusion protein and expressed in *G. oxydans* and the phosphatase activity was measured. Rate of PhoA activity was monitored as $\Delta A_{405\ nm}/(h \times OD_{600\ nm})$. Letters above the plot denote statistical groups determined by an ANOVA and post-hoc Tukey's HSD test. Full-size DOI: 10.7717/peerj.4626/fig-5

led to a statistically significant increase in mean doubling time (97 min) compared to wildtype cells (56 min) ($q < 0.001$) (Fig. 7). However, when the OprF188-PhoA fusion was expressed, the doubling time (52 min) was not different than that of wildtype cells ($q = 0.603$). The presence of the small FL (FL1) increased the doubling time (82 min) compared to the strain expressing the OprF188-PhoA fusion without a linker ($q < 0.001$). Conversely, the presence of the small RL (RL1) decreased doubling time (27 min) compared to the strain lacking the linker ($q < 0.001$) and to wildtype cells ($q < 0.001$). However, the lag time for this strain was approximately 8 h longer than that of wildtype cells (Fig. 6). The medium RL (RL2) did not affect doubling time (58 min) compared to the no-linker control strain ($q = 0.166$) or wildtype cells ($q = 0.952$) (Fig. 7). Lastly, the large RL (RL3) increased doubling time to 121 min. Generally, the lag time was longer for recombinant strains and the final optical density was lower than that of wildtype *G. oxydans*, except for the p264-oprF-RL1-phoA containing strain (Fig. 6) that also produced the highest PhoA activity. Interestingly, doubling time was inversely proportional to PhoA activity (Figs. 5 and 7, respectively), suggesting that recombinant PhoA positively contributed to the growth of *G. oxydans*.

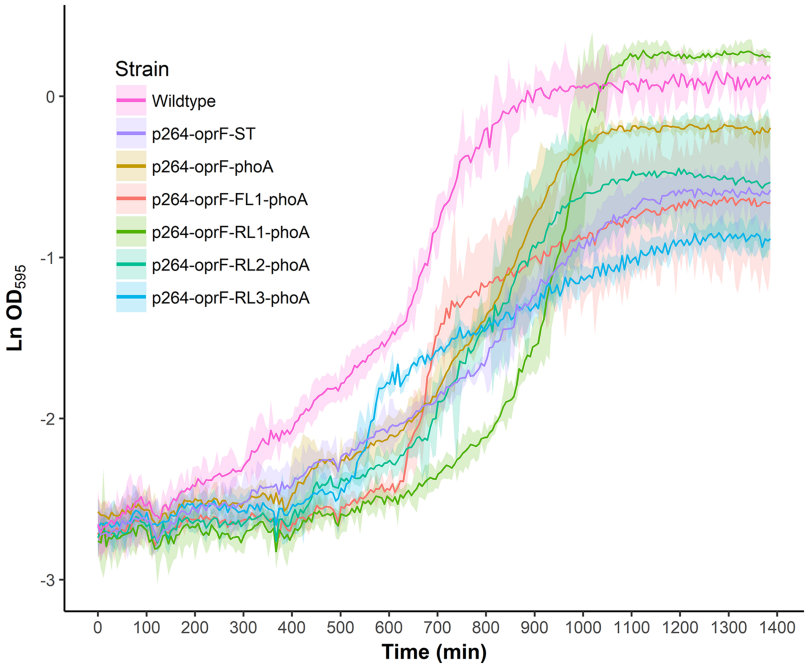

Figure 6 Growth behavior of recombinant *G. oxydans* strains. Cells were cultured in 24-well microplates and the growth of recombinant *G. oxydans* 621H strains was compared to that of wildtype. Solid line, mean optical density; ribbon, 95% CI; $n = 3$. Full-size DOI: 10.7717/peerj.4626/fig-6

DISCUSSION

In this study, the gene encoding PhoA was fused to OprF188 to test the ability of the anchor peptide to transport recombinant enzymes to the cell surface of acetic acid bacteria. The resulting constructs were expressed in the model acetic acid bacterium *G. oxydans* and biocatalysis was quantified in whole-cell reactions. Based on enzymatic activity, OprF188 localized active PhoA to the cell surface, regardless of expression level. Nascent PhoA has no activity in the cytoplasm as it does not fold properly unless secreted extracellularly where disulfide bonding takes place (*De Geyter et al., 2016*; *Ehrmann, Boyd & Beckwith, 1990*; *Hoffman & Wright, 1985*; *Manoil & Beckwith, 1985*; *Michaelis et al., 1983*). The native periplasmic signal sequence was removed from PhoA before it was fused to OprF188, which contains an outer membrane signal peptide and is known to localize to the outer membrane (*Lee et al., 2005*; *Sugawara, Nagano & Nikaido, 2012*). The OprF188-PhoA fusion was produced using two expression vectors designed for protein production in *G. oxydans*, one containing a high-strength p264 promoter, and the other a moderate-strength p452 promoter. There was a twofold difference in phosphatase activity produced by *G. oxydans* between the two promoters. This mirrors the threefold difference in enzymatic activity reported previously (*Kallnik et al., 2010*).

Because PhoA is an innately periplasmic enzyme, its location needed to be verified to show that OprF188 can correctly target recombinant enzymes to the outer leaflet of the outer membrane in *G. oxydans*. To this end, a CL was integrated between OprF188 and PhoA as was done previously to validate another surface display systems (*Jiang & Boder, 2010*). If PhoA was exposed at the cell surface via OprF188, then PhoA should be

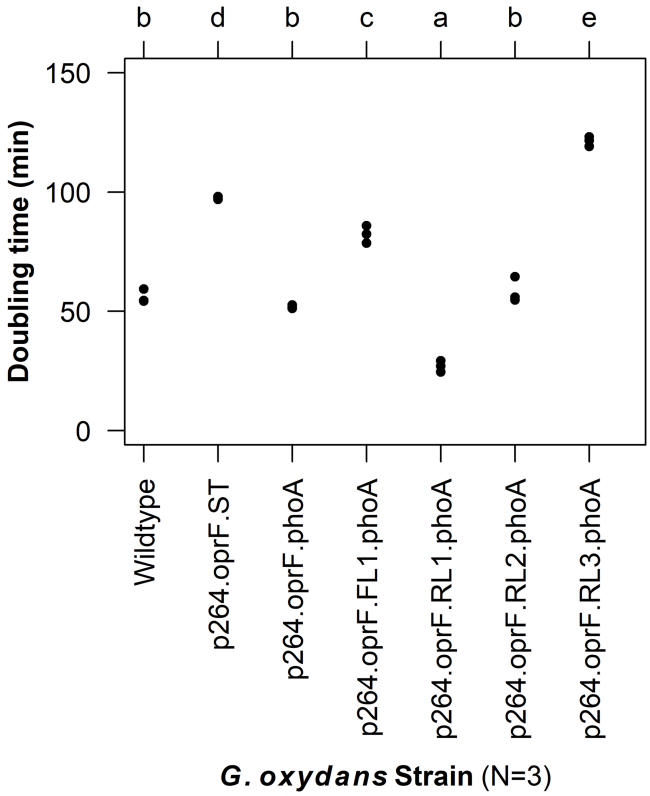

Figure 7 Doubling time of *G. oxydans* strains. Doubling time was calculated using the growthcurver R package. Letters above the plot denote statistical groups determined by an ANOVA and post-hoc Tukey's HSD test. Full-size DOI: 10.7717/peerj.4626/fig-7

removed from the outer membrane following treatment with Factor Xa protease, increasing phosphatase activity in the medium. The CL assay demonstrated that the level of phosphatase activity in the treated supernatant fractions was indeed higher than that in the untreated supernatant fractions ($p < 0.001$), which suggests that PhoA was present at the outer leaflet of the outer membrane.

In this study, we used a C-terminal truncated version of OprF, OprF188, containing 188 amino acids from the N-terminus of the original protein in its mature form. Valine 188 was previously determined to be the optimal fusion site for passenger proteins (*Lee et al., 2005*). This anchor protein was previously used to localize a 49.9 kDa lipase, which is comparable to the size of the 47 kDa PhoA monomer (*Bradshaw et al., 1981*), to the outer membrane of *E. coli* (*Lee et al., 2005*) and *Pseudomonas putida* (*Lee, Lee & Park, 2005*). The first 24 amino acids of nascent OprF188 encodes a Sec-dependent signal peptide. OprF is an unusual outer membrane protein in that it is comprised of two domains: An N-terminal domain that forms a small, eight-stranded β-barrel, and a C-terminal globular domain that associates with the cell wall in the periplasm (*Bodilis & Barray, 2006*; *Sugawara, Nagano & Nikaido, 2012*). Mature OprF188 consists of only the β-barrel domain with a C-terminal extracellular loop (*Lee et al., 2005*). OprF is also unusual because the β-signal that is recognized by the β-barrel assembly complex to facilitate outer membrane integration, is located internally at the end of the β-barrel domain, rather than

C-terminally (*Gessmann et al., 2014*; *Sugawara, Nagano & Nikaido, 2012*). Thus, truncated OprF188 maintains its β-signal, allowing proper membrane integration (*Lee et al., 2005*; *Sugawara, Nagano & Nikaido, 2012*).

Interestingly, there have been many unsuccessful attempts to target PhoA to the cell surface of *E. coli* using *E. coli* outer membrane proteins as anchors. PhoA was fused to the ferrichrome outer membrane transporter FhuA (*Coulton, Reid & Campana, 1988*). While PhoA was associated with the outer membrane, it was not necessarily exposed to the outer surface. Similarly, the ferric enterobactin outer membrane transporter FepA localized PhoA to the outer membrane of *E. coli*, but it was periplasmically oriented (*Murphy & Klebba, 1989*). When a PhoA was fused to a lipoprotein-OmpA hybrid, again the fusion protein was associated with the outer membrane but PhoA existed exclusively in the periplasm (*Stathopoulos, Georgiou & Earhart, 1996*). Close inspection of these studies reveals that the β-signal was removed from FhuA, FepA, and OmpA upon C-terminal truncation. Therefore, deletion of the β-signal was likely sufficient to prevent proper outer membrane insertion by the β-barrel assembly complex in those studies. The use of OprF188 as an anchor to successfully display proteins on the cell surface in the current study and by others suggests that it is broadly functional as a surface display anchor protein in gram-negative bacteria, likely due to the preservation of the β-signal (*Lee et al., 2005*; *Lee, Lee & Park, 2005*).

Despite their influence on fusion protein activity, the effect of linkers on bacterial surface display has not previously been investigated. While linkers are sometimes included in the design of surface display systems, their inclusion is rarely made explicit and even fewer studies offer any explanation as to why a particular linker sequence was chosen. Yet linker sequences can play a vital role in the design of fusion proteins, affecting protein folding and production efficiency, and influencing enzyme activity (*Chen, Zaro & Shen, 2013*; *Li et al., 2016*). Here, a library of linkers varying in both composition and length were integrated into a surface display system to explicitly test the effects of linkers on biocatalysis at the cell surface of two bacterial species. Two types of linkers were investigated in this study, FLs and RLs. FLs are composed of small, polar amino acids such as glycine and serine and form random coils, such as the $(GGGGS)_{1–3}$ linker used here. RLs are often α-helical, such as the $(EAAAK)_{1–3}$ linker used here (*Chen, Zaro & Shen, 2013*; *Li et al., 2016*). FLs provide passive separation and permit interaction between the components of fusion proteins, while RLs maintain a set distance and can prevent interaction between fusion protein domains (*Li et al., 2016*). The linker library was first expressed in *E. coli* and, generally, the presence of linkers did not dramatically influence product yield. In contrast, the linkers caused pronounced effects on biocatalysis in *G. oxydans*. Fusion proteins containing the medium (FL2) and large (FL3) FLs—10 and 15 amino acids in length—were likely toxic to *G. oxydans*, as positive transformants were not obtained after multiple attempts. The fusion proteins containing the small flexible (FL1) and medium rigid (RL2) linkers had no influence on biocatalysis, whereas the large rigid (RL3) linker was deleterious. Optimization of the surface display system was achieved with the small RL (RL1), consisting of a single EAAAK pentapeptide, which improved phosphatase activity by 69%.

The disparate results of the linkers on *E. coli* and *G. oxydans* suggest that the effects of linkers on biocatalysis at the cell surface may be species-specific. *E. coli* and *G. oxydans* are phylogenetically distant, belonging to the *Gammaproteobacteria* and *Alphaproteobacteria*, respectively. There are likely differences in the composition of their outer membranes and thus the environment at the cell surface of these bacteria. It should be noted that the outer membrane composition of *G. oxydans* and other acetic acid bacteria remains largely uncharacterized, limiting direct comparison. Nevertheless, these differences may also be why phosphatase activity was overall higher in *E. coli* than in *G. oxydans*. Differences in promoter strength and/or efficiency of secretion (*Choi & Lee, 2004*) or outer membrane protein assembly by the β-barrel assembly complex (*Browning et al., 2015*; *Sikora et al., 2017*) may also play a role in the differences in the activities observed between *E. coli* and *G. oxydans*. Additionally, the differences in linker effects could also be passenger protein-specific. Overall, these results suggest that linker optimization is an important consideration for each surface display system used and for the specific host organism.

To determine the effects of protein production and surface engineering on the growth of *G. oxydans*, a novel method was developed for semi-high-throughput culturing of *G. oxydans*. The strain containing plasmid p264-oprF-ST had significantly slower growth compared to wildtype *G. oxydans* 621H. It is possible that this growth defect was caused by the metabolic burden of protein production. Alternatively, the production of the OprF188 peptide may have overwhelmed secretory machinery, preventing sufficient amounts of required proteins from being processed. It is also possible that integration of the OprF188 anchor destabilizes outer membrane integrity. Interestingly, the p264-oprF-phoA strain did not exhibit a growth defect, suggesting that PhoA may enable recovery of the OprF188 phenotype. It may be that high expression of PhoA allowed cells to scavenge more phosphate from the medium, possibly allowing recovery from outer membrane lipid defects. Indeed, the small RL (RL1) not only increased PhoA activity, but also improved the growth rate with concomitant increased lag time. PhoA activity seemed to be inversely proportional with doubling time, suggesting that inorganic phosphate availability may contribute to the observed growth phenotypes.

CONCLUSION

Surface display is potentially a powerful tool to enable metabolic engineering of *G. oxydans* and other industrially important acetic acid bacteria. *G. oxydans* currently has a limited ability to grow on disaccharides and polysaccharides, and instead relies on relatively expensive monomeric feedstocks (*Kosciow et al., 2016*). The ability to express enzymes at the outer membrane could be used to improve current bioprocesses by broadening the substrate range of this bacterium. Because this technique utilizes export machinery found in all gram-negative bacteria, the surface display constructs could be expressed in otherwise wildtype cells. Previously, a recombinant exoenzyme with a periplasmic signal peptide was efficiently released from cells only when a knockout strain of *G. oxydans* with a leaky outer membrane phenotype was used (*Kosciow et al., 2016*). Surface display could also be used in conjunction with immobilized *G. oxydans* cells to create stable bioreactors, such as those used in the production of dihydroxyacetone

(*Dikshit & Moholkar, 2016*). In conclusion, a novel molecular tool for strain improvement of acetic acid bacteria was produced, and the OprF188 surface display system described herein is a significant first step toward outer membrane engineering of *G. oxydans*. Such molecular tools will enable engineering of this unique bacterium to improve and expand its ability to produce value-added products.

ACKNOWLEDGEMENTS

We thank Dr. Kyoungtae Kim and Dr. Laszlo Kovacs for lending their expertise and providing feedback on this project.

ADDITIONAL INFORMATION AND DECLARATIONS

Funding

This work was supported by funds from the Missouri State University Biology Department and the Graduate College. The funders had no role in study design, data collection and analysis, decision to publish, or preparation of the manuscript.

Grant Disclosures

The following grant information was disclosed by the authors:
Missouri State University Biology Department and the Graduate College.

Competing Interests

The authors declare that they have no competing interests.

Author Contributions

- Marshal Blank conceived and designed the experiments, performed the experiments, analyzed the data, contributed reagents/materials/analysis tools, prepared figures and/or tables, authored or reviewed drafts of the paper, approved the final draft.
- Paul Schweiger conceived and designed the experiments, analyzed the data, contributed reagents/materials/analysis tools, prepared figures and/or tables, authored or reviewed drafts of the paper, approved the final draft.

Data Availability

The following information was supplied regarding data availability:

The raw data that was used to generate statistics/error bars and corresponding R code for each figure are available as Supplemental Files.

Supplemental Information

Supplemental information for this article can be found online at http://dx.doi.org/10.7717/peerj.4626#supplemental-information.

REFERENCES

Bodilis J, Barray S. 2006. Molecular evolution of the major outer-membrane protein gene (oprF) of pseudomonas. *Microbiology* **152(4)**:1075–1088 DOI 10.1099/mic.0.28656-0.

Bradshaw RA, Cancedda F, Ericsson LH, Neumann PA, Piccoli SP, Schlesinger MJ, Shriefer K, Walsh KA. 1981. Amino acid sequence of *Escherichia coli* alkaline phosphatase. *Proceedings of the National Academy of Sciences of the United States of America* **78(6)**:3473–3477 DOI 10.1073/pnas.78.6.3473.

Browning DF, Bavro VN, Mason JL, Sevastsyanovich YR, Rossiter AE, Jeeves M, Wells TJ, Knowles TJ, Cunningham AF, Donald JW, Palmer T, Overduin M, Henderson IR. 2015. Cross-species chimeras reveal BamA POTRA and beta-barrel domains must be fine-tuned for efficient OMP insertion. *Molecular Microbiology* **97(4)**:646–659 DOI 10.1111/mmi.13052.

Chen X, Zaro JL, Shen WC. 2013. Fusion protein linkers: property, design and functionality. *Advanced Drug Delivery Reviews* **65(10)**:1357–1369 DOI 10.1016/j.addr.2012.09.039.

Choi JH, Lee SY. 2004. Secretory and extracellular production of recombinant proteins using *Escherichia coli*. *Applied Microbiology and Biotechnology* **64(5)**:625–635 DOI 10.1007/s00253-004-1559-9.

Coulton JW, Reid GK, Campana A. 1988. Export of hybrid proteins FhuA′-′LacZ and FhuA′-′PhoA to the cell envelope of *Escherichia coli* K-12. *Journal of Bacteriology* **170(5)**:2267–2275 DOI 10.1128/jb.170.5.2267-2275.1988.

De Geyter J, Tsirigotaki A, Orfanoudaki G, Zorzini V, Economou A, Karamanou S. 2016. Protein folding in the cell envelope of *Escherichia coli*. *Nature Microbiology* **1(8)**:16107 DOI 10.1038/nmicrobiol.2016.107.

De Muynck C, Pereira CS, Naessens M, Parmentier S, Soetaert W, Vandamme EJ. 2007. The genus *Gluconobacter oxydans*: comprehensive overview of biochemistry and biotechnological applications. *Critical Reviews in Biotechnology* **27(3)**:147–171 DOI 10.1080/07388550701503584.

Deppenmeier U, Ehrenreich A. 2009. Physiology of acetic acid bacteria in light of the genome sequence of *Gluconobacter oxydans*. *Journal of Molecular Microbiology and Biotechnology* **16(1–2)**:69–80 DOI 10.1159/000142895.

Deppenmeier U, Hoffmeister M, Prust C. 2002. Biochemistry and biotechnological applications of Gluconobacter strains. *Applied Microbiology and Biotechnology* **60(3)**:233–242 DOI 10.1007/s00253-002-1114-5.

Dikshit PK, Moholkar VS. 2016. Kinetic analysis of dihydroxyacetone production from crude glycerol by immobilized cells of *Gluconobacter oxydans* MTCC 904. *Bioresource Technology* **216**:948–957 DOI 10.1016/j.biortech.2016.06.042.

Ehrmann M, Boyd D, Beckwith J. 1990. Genetic analysis of membrane protein topology by a sandwich gene fusion approach. *Proceedings of the National Academy of Sciences of the United States of America* **87(19)**:7574–7578 DOI 10.1073/pnas.87.19.7574.

Gessmann D, Chung YH, Danoff EJ, Plummer AM, Sandlin CW, Zaccai NR, Fleming KG. 2014. Outer membrane beta-barrel protein folding is physically controlled by periplasmic lipid head groups and BamA. *Proceedings of the National Academy of Sciences of the United States of America* **111(16)**:5878–5883 DOI 10.1073/pnas.1322473111.

Guigas G, Weiss M. 2016. Effects of protein crowding on membrane systems. *Biochimica et Biophysica Acta (BBA)–Biomembranes* **1858(10)**:2441–2450 DOI 10.1016/j.bbamem.2015.12.021.

Hoffman CS, Wright A. 1985. Fusions of secreted proteins to alkaline phosphatase: an approach for studying protein secretion. *Proceedings of the National Academy of Sciences of the United States of America* **82(15)**:5107–5111 DOI 10.1073/pnas.82.15.5107.

Hothorn T, Bretz F, Westfall P. 2008. Simultaneous inference in general parametric models. *Biometrical Journal* **50(3)**:346–363 DOI 10.1002/bimj.200810425.

Jiang W, Boder ET. 2010. High-throughput engineering and analysis of peptide binding to class II MHC. *Proceedings of the National Academy of Sciences of the United States of America* **107(30)**:13258–13263 DOI 10.1073/pnas.1006344107.

Kallnik V, Meyer M, Deppenmeier U, Schweiger P. 2010. Construction of expression vectors for protein production in *Gluconobacter oxydans*. *Journal of Biotechnology* **150(4)**:460–465 DOI 10.1016/j.jbiotec.2010.10.069.

Kosciow K, Domin C, Schweiger P, Deppenmeier U. 2016. Extracellular targeting of an active endoxylanase by a TolB negative mutant of *Gluconobacter oxydans*. *Journal of Industrial Microbiology & Biotechnology* **43(7)**:989–999 DOI 10.1007/s10295-016-1770-6.

Kosciow K, Zahid N, Schweiger P, Deppenmeier U. 2014. Production of a periplasmic trehalase in *Gluconobacter oxydans* and growth on trehalose. *Journal of Biotechnology* **189**:27–35 DOI 10.1016/j.jbiotec.2014.08.029.

Kostner D, Peters B, Mientus M, Liebl W, Ehrenreich A. 2013. Importance of codB for new codA-based markerless gene deletion in Gluconobacter strains. *Applied Microbiology and Biotechnology* **97(18)**:8341–8349 DOI 10.1007/s00253-013-5164-7.

Lee SH, Choi JI, Han MJ, Choi JH, Lee SY. 2005. Display of lipase on the cell surface of *Escherichia coli* using OprF as an anchor and its application to enantioselective resolution in organic solvent. *Biotechnology and Bioengineering* **90(2)**:223–230 DOI 10.1002/bit.20399.

Lee SH, Lee SY, Park BC. 2005. Cell surface display of lipase in Pseudomonas putida KT2442 using OprF as an anchoring motif and its biocatalytic applications. *Applied and Environmental Microbiology* **71(12)**:8581–8586 DOI 10.1128/AEM.71.12.8581-8586.2005.

Li G, Huang Z, Zhang C, Dong BJ, Guo RH, Yue HW, Yan LT, Xing XH. 2016. Construction of a linker library with widely controllable flexibility for fusion protein design. *Applied Microbiology and Biotechnology* **100(1)**:215–225 DOI 10.1007/s00253-015-6985-3.

Manoil C, Beckwith J. 1985. TnphoA: a transposon probe for protein export signals. *Proceedings of the National Academy of Sciences of the United States of America* **82(23)**:8129–8133 DOI 10.1073/pnas.82.23.8129.

Michaelis S, Inouye H, Oliver D, Beckwith J. 1983. Mutations that alter the signal sequence of alkaline phosphatase in *Escherichia coli*. *Journal of Bacteriology* **154(1)**:366–374.

Murphy CK, Klebba PE. 1989. Export of FepA::PhoA fusion proteins to the outer membrane of *Escherichia coli* K-12. *Journal of Bacteriology* **171(11)**:5894–5900 DOI 10.1128/jb.171.11.5894-5900.1989.

Nagai K, Thogersen HC. 1987. Synthesis and sequence-specific proteolysis of hybrid proteins produced in *Escherichia coli*. *Methods in Enzymology* **153**:461–481 DOI 10.1016/0076-6879(87)53072-5.

Olijve W, Kok JJ. 1979. An analysis of growth of *Gluconobacter oxydans* in chemostat cultures. *Archives of Microbiology* **121(3)**:291–297 DOI 10.1007/bf00425070.

Pappenberger G, Hohmann HP. 2014. Industrial production of L-ascorbic Acid (vitamin C) and D-isoascorbic acid. *Advances in Biochemical Engineering/Biotechnology* **143**:143–188 DOI 10.1007/10_2013_243.

Peters B, Junker A, Brauer K, Muhlthaler B, Kostner D, Mientus M, Liebl W, Ehrenreich A. 2013. Deletion of pyruvate decarboxylase by a new method for efficient markerless gene deletions in *Gluconobacter oxydans*. *Applied Microbiology and Biotechnology* **97(6)**:2521–2530 DOI 10.1007/s00253-012-4354-z.

Prust C, Hoffmeister M, Liesegang H, Wiezer A, Fricke WF, Ehrenreich A, Gottschalk G, Deppenmeier U. 2005. Complete genome sequence of the acetic acid bacterium *Gluconobacter oxydans*. *Nature Biotechnology* **23(2)**:195–200 DOI 10.1038/nbt1062.

Raspor P, Goranovic D. 2008. Biotechnological applications of acetic acid bacteria. *Critical Reviews in Biotechnology* **28(2)**:101–124 DOI 10.1080/07388550802046749.

R Core Team. 2017. *R: A Language and Environment for Statistical Computing*. Vienna: R Foundation for Statistical Computing. *Available at https://www.R-project.org/*.

Schedel M. 2000. *Oxidation of Aminosorbitol with Gox in Synthesis of Deoxynojirimycin*. Weinheim: Wiley-VHC.

Schüürmann J, Quehl P, Festel G, Jose J. 2014. Bacterial whole-cell biocatalysts by surface display of enzymes: toward industrial application. *Applied Microbiology and Biotechnology* **98(19)**:8031–8046 DOI 10.1007/s00253-014-5897-y.

Shi L, Li K, Zhang H, Liu X, Lin J, Wei D. 2014. Identification of a novel promoter gHp0169 for gene expression in *Gluconobacter oxydans*. *Journal of Biotechnology* **175**:69–74 DOI 10.1016/j.jbiotec.2014.01.035.

Sikora AE, Wierzbicki IH, Zielke RA, Ryner RF, Korotkov KV, Buchanan SK, Noinaj N. 2017. Structural and functional insights into the role of BamD and BamE within the β-barrel assembly machinery in *Neisseria gonorrhoeae*. *Journal of Biological Chemistry* **293(4)**:1106–1119 DOI 10.1074/jbc.RA117.000437.

Sprouffske K, Wagner A. 2016. Growthcurver: an R package for obtaining interpretable metrics from microbial growth curves. *BMC Bioinformatics* **17(1)**:172 DOI 10.1186/s12859-016-1016-7.

Stathopoulos C, Georgiou G, Earhart CF. 1996. Characterization of *Escherichia coli* expressing an Lpp'OmpA(46-159)-PhoA fusion protein localized in the outer membrane. *Applied Microbiology and Biotechnology* **45(1–2)**:112–119 DOI 10.1007/s002530050657.

Sugawara E, Nagano K, Nikaido H. 2012. Alternative folding pathways of the major porin OprF of *Pseudomonas aeruginosa*. *FEBS Journal* **279(6)**:910–918 DOI 10.1111/j.1742-4658.2012.08481.x.

Terpe K. 2003. Overview of tag protein fusions: from molecular and biochemical fundamentals to commercial systems. *Applied Microbiology and Biotechnology* **60(5)**:523–533 DOI 10.1007/s00253-002-1158-6.

Voss J, Ehrenreich A, Liebl W. 2010. Characterization and inactivation of the membrane-bound polyol dehydrogenase in *Gluconobacter oxydans* DSM 7145 reveals a role in meso-erythritol oxidation. *Microbiology* **156(6)**:1890–1899 DOI 10.1099/mic.0.037598-0.

Wickham H. 2007. Reshaping Data with the reshape Package. *Journal of Statistical Software* 21**(12)**:1–20 DOI 10.18637/jss.v021.i12.

Wickham H. 2009. *ggplot2: Elegant Graphics for Data Analysis*. New York: Springer-Verlag.

Wickham H. 2011. The Split-Apply-Combine Strategy for Data Analysis. *Journal of Statistical Software* 40**(1)**:1–29 DOI 10.18637/jss.v040.i01.

Wickham H, Francois R, Henry L, Müller K. 2017. *dplyr: A Grammar of Data Manipulation*. R package version 0.7.3. *Available at https://CRAN.R-project.org/package=dplyr*.

Yang W, Xu H. 2016. Industrial fermentation of vitamin C. In: Revuelta JL, Vandamme EJ, eds. *Industrial Biotechnology of Vitamins, Biopigments, and Antioxidants*. Germany: Wiley-VCH Verlag GmbH & Co. KGaA, 161–192.

Zeiser J, Mühlenbeck LH, Schweiger P, Deppenmeier U. 2014. Characterization of a periplasmic quinoprotein from *Sphingomonas wittichii* that functions as aldehyde dehydrogenase. *Applied Microbiology and Biotechnology* **98(5)**:2067–2079 DOI 10.1007/s00253-013-5016-5.

Zhang L, Lin J, Ma Y, Wei D, Sun M. 2010. Construction of a novel shuttle vector for use in *Gluconobacter oxydans*. *Molecular Biotechnology* **46(3)**:227–233 DOI 10.1007/s12033-010-9293-2.